

A universal framework for route diversification in road networks

Giuliano Cornacchia^{1,2}, Luca Pappalardo^{1,3}, Mirco Nanni¹, Dino Pedreschi², Marta C. González^{4, 5, 6}

¹ISTI-CNR, Pisa, Italy

²University of Pisa, Pisa, Italy

³Scuola Normale Superiore of Pisa, Italy

⁴Department of City and Regional Planning, University of California, Berkeley, CA, USA

⁵Energy Technologies Area, Lawrence Berkeley National Laboratory, Berkeley, CA, USA

⁶Department of Civil and Environmental Engineering, University of California, Berkeley, CA, USA

1 The structure of road networks significantly impacts various urban dynamics, from traffic
2 congestion to environmental sustainability and equitable access to services. Recent studies
3 reveal that most roads are underutilized, faster alternative routes are often overlooked, and
4 traffic is typically concentrated on a few corridors. In this article, we examine how road net-
5 work topology, and in particular the presence of mobility attractors (e.g., highways and ring
6 roads), shapes the counterpart to traffic concentration: route diversification. To this end,
7 we introduce DiverCity, a measure that quantifies the extent to which traffic can potentially
8 be distributed across multiple, loosely overlapping routes. Analyzing 56 global cities with
9 diverse population densities and road network topologies, we find that DiverCity is closely
10 tied to traffic efficiency and network characteristics such as network extensiveness and num-
11 ber of intersections. Within cities, DiverCity increases with distance from the city center
12 before stabilizing in the periphery but declines in the proximity of mobility attractors. We
13 demonstrate that strategic speed limit adjustments on mobility attractors can increase Di-
14 verCity while preserving travel efficiency. We isolate the complex interplay between mobility
15 attractors and DiverCity through simulations in a controlled setting, confirming the patterns
16 observed in real-world cities. DiverCity provides a practical tool for urban planners and
17 policymakers to optimize road network design and balance route diversification, efficiency,
18 and sustainability. We provide an interactive platform (<https://divercitymaps.github.io>) to
19 visualize the spatial distribution of DiverCity across all considered cities.

20 **Introduction**

21 The structure of road networks profoundly influences essential aspects of urban life, such as traffic
22 congestion^{1–3}, environmental sustainability^{4–7}, land use patterns⁸, the spatial organization of cities
23^{9,10}, and equitable access to essential services and amenities^{11,12}. Recent findings reveal substantial
24 inefficiencies in how drivers use road networks: an estimated 98% of roads are underutilized^{13,14},
25 16% of highway-based routes have quicker alternatives¹⁵, and traffic is typically concentrated into
26 a limited number of corridors^{2,16–18}. The growing reliance on GPS-based navigation services like
27 TomTom and Google Maps may further amplify these inefficiencies, as both anecdotal evidence
28^{19–21} and recent studies suggest^{22–26}.

29 Traffic concentration arises from the interplay between the road network's structure – en-
30 abling or constraining efficient traffic distribution – and mobility dynamics, shaped by how pop-
31ulations are dispersed and the associated travel demand. In this article, we investigate the role of
32 network topology – and particularly the presence of mobility attractors such as highways and ring
33 roads, which are typically preferred by drivers – in shaping the dual of traffic concentration: route
34 diversification. By potential route diversification, we mean the extent to which traffic can poten-
35 tially be distributed across multiple, loosely overlapping routes. How do road networks vary in
36 their capacity for route diversification, and how can these differences be measured? Which factors
37 drive or hinder route diversification, and what role do mobility attractors play? Finally, can route
38 diversification in road networks be effectively guided through non-disruptive policy interventions?

39 A review of the literature reveals a critical gap: no existing measure quantifies potential route
40 diversification in road networks, leaving these fundamental questions unanswered. On the one
41 hand, edge-level metrics – such as betweenness centrality and K_{road} – provide insights into network
42 flow but are hardly generalizable at the route level. Betweenness centrality²⁷ quantifies how many
43 shortest routes pass through an edge, ignoring the range of near-shortest alternatives that drivers
44 may realistically take. K_{road} ¹³ quantifies the contribution of different city areas to edge-level traffic
45 but cannot assess the diversity of routes available between an origin and a destination. On the other

46 hand, route-level metrics also fall short. The detour index^{28–30} measures how much a route deviates
47 from its straight-line distance but does not account for alternative routes between the origin and
48 destination. Similarly, the inness measure³¹ evaluates whether routes tend to converge toward or
49 diverge from the city center but focuses only on the shortest and fastest paths, overlooking route
50 diversity.

51 We fill this gap by introducing DiverCity, a measure that quantifies both the number of practical alternative routes – those only marginally longer than the fastest path – and their spatial overlap.
52 Our measure relies exclusively on road network data, making it applicable to any city and enabling
53 a direct assessment of how network topology influences potential route diversification. To ensure
54 independence from actual travel demand, we employ the state-of-the-art radial sampling method
55 that generates origin-destination pairs at varying distances from the city center, guaranteeing con-
56 sistency across all cities analyzed. We then apply DiverCity to 56 cities worldwide, each covering
57 a 30 km radius from the city center, spanning all six inhabited continents, varying population
58 densities, and diverse road network structures.

60 We observe substantial variability in potential route diversification across cities. Tokyo ex-
61 hibits the highest DiverCity, while Mumbai shows the lowest, with a potential route diversifica-
62 tion approximately 38% lower than Tokyo's. Between these two extremes, cities display a wide
63 spectrum of route diversification levels, with grid-structured cities (like Chicago and New York)
64 exhibiting higher DiverCity compared to non-gridded counterparts (like Brussels and Istanbul).
65 Notably, we find that DiverCity is strongly linked to traffic efficiency: cities with higher potential
66 route diversification allow for a more balanced distribution of vehicular traffic. DiverCity is also
67 correlated with key road network characteristics: cities with more extensive road networks, higher
68 number of intersections, and fewer indirect paths exhibit greater route diversification.

69 The spatial analysis of DiverCity within cities reveals a universal pattern: it increases with
70 distance from the city center and plateaus in peripheral areas. Mobility attractors, such as highways
71 and ring roads, play a pivotal role in shaping this distribution. We find that DiverCity consistently

72 decreases near these attractors as they funnel traffic into fast corridors, limiting the use of alter-
73 native routes thereby reducing diversification for trips in their immediate vicinity. However, our
74 results reveal that when strategically spaced and well-distributed, mobility attractors may enhance
75 DiverCity at a city-wide scale. For example, in Rome, mobility attractors are poorly distributed,
76 and they reduce potential route diversification considerably; in Tokyo, mobility attractors are dense
77 and well-distributed, minimizing local suppressive effects and stabilizing DiverCity across the city.

78 We propose speed limit tuning as a targeted intervention to counteract the observed sup-
79 pressive effects of mobility attractors. We demonstrate that moderate speed reductions mitigate
80 attractors' dominance, increasing potential route diversification considerably with only a minimal
81 impact on travel times. To model the impact of mobility attractors on DiverCity and uncover the
82 mechanisms that govern it, we develop a controlled simulation on a simplified road network rep-
83 resentation. This synthetic road network replicates a grid-structured city with a 30 km radius,
84 matching real-world cases. Within this framework, we vary the spatial distribution and speed
85 limits of mobility attractors to analyze their impact on DiverCity. Our results closely align with
86 real-world observations, confirming both the local and global effects of mobility attractors and
87 demonstrating the effectiveness of speed limit reductions in mitigating their impact on potential
88 route diversification.

89 Our study equips city planners, policymakers, and transportation authorities with valuable
90 tools to promote more efficient use of the road network. DiverCity can guide infrastructure in-
91 vestments by pinpointing areas that would benefit from new road connections or speed limit ad-
92 justments. Our measure can also aid in preliminary impact assessments of urban policies like the
93 30 km/h speed limits policy^{32,33} by identifying how potential route diversification would respond
94 to changes in speed regulations. As a further contribution, we provide an interactive online plat-
95 form (<https://divercitymaps.github.io>) to visualize the spatial distribution of DiverCity across all
96 considered cities.

97 **Measuring potential route diversification**

98 We quantify a trip's potential route diversification (trip DiverCity) by examining the geographical
99 characteristics of the alternative routes connecting its origin and destination. Mathematically, we
100 define the DiverCity of a trip (u, v) as:

101
$$\mathcal{D}(u, v) = \mathcal{S}(\text{NSR}(u, v)) \cdot |\text{NSR}(u, v)| \quad (1)$$

102 where $\text{NSR}(u, v)$ is the set of near-shortest routes between locations u and v , and $\mathcal{S}(\text{NSR}(u, v))$
103 represents their spatial spread.

104 By near-shortest routes, we refer to alternative routes whose cost deviates only slightly from
105 that of the fastest route. These represent the practical alternatives that drivers are most likely
106 to consider when traveling to their destination. To identify near-shortest routes, we generate up
107 to k alternative routes for a trip using path penalization^{34–38} (see Methods for details). We set
108 $k = 10$ based on empirical evidence indicating that drivers' route choices are typically limited to
109 10 options³⁹. In Supplementary Note 1, we demonstrate that the results presented in this study
110 remain robust for $k \in [2, 15]$.

111 Regarding the spatial spread, $\mathcal{S}(\text{NSR}(u, v)) = 1 - J(\text{NSR}(u, v))$, where J is the average
112 weighted Jaccard similarity among all pairs of routes in $\text{NSR}(u, v)$ (see Methods for details).
113 $\mathcal{S}(\text{NSR}(u, v))$, captures the geographical diversity of near-shortest routes between u and v , re-
114 lying on empirical evidence indicating that drivers' route choices are typically constrained within
115 well-defined spatial boundaries³⁹. A high $\mathcal{S}(\text{NSR}(u, v))$ indicates minimal overlap among the
116 routes. A low $\mathcal{S}(\text{NSR}(u, v))$ suggests that the near-shortest routes are highly similar, deviating
117 only slightly from the fastest route.

118 $\mathcal{D}(u, v)$ ranges in $[0, k]$, where a trip with only one route has $\mathcal{D}(u, v) = 0$ and a trip with
119 k disjoint near-shortest routes has $\mathcal{D}(u, v) = k$. Note that trip DiverCity is not symmetric, i.e.,
120 $\mathcal{D}(u, v) \neq \mathcal{D}(v, u)$, because of the possible existence of one-way streets between the two locations.
121 Figure 1a and 1b compare two trips of equal origin-to-destination distance (≈ 24 km) in Mumbai

122 and Tokyo. The trip in Mumbai has six near-shortest routes (in blue) alongside four excessively
123 long alternatives (in red), see Figure 1a. The concentration of routes leads to substantial overlap,
124 yielding a low $\mathcal{D}_{\text{Mumbai}}(u, v) = 2.18$. In contrast, the trip in Tokyo has many near-shortest routes
125 with a low spatial overlap, resulting in a high $\mathcal{D}_{\text{Tokyo}}(u, v) = 9$ (see Figure 1b).

126 We analyze 56 cities worldwide downloading publicly available road networks from Open-
127 StreetMap⁴⁰, each covering a 30 km radius from the city center. These cities span multiple con-
128 tinents, varying population densities, and diverse road network structures (see Table 1 for the list
129 of cities considered and their characteristics). For each city, we create a set of trips T using the
130 radial sampling method³¹, which draws concentric circles at various distances from the city center.
131 The endpoints of trips in T (sampled nodes) correspond to intersections in the road network. This
132 approach ensures that each trip's origin and destination lie on the same circle (see Methods for
133 details) and effectively captures real mobility flow patterns in urban environments^{29,31}. By em-
134 ploying radial sampling, our analysis depends solely on road network information, eliminating the
135 need for real mobility data and avoiding biases from real origin-destination matrices. This yields a
136 purely topological perspective on potential route diversification.

137 Results

138 For each city C , we define the city-level DiverCity as the median trip DiverCity across trips in T ,
139 expressed as $\mathcal{D}_C = \text{median}\{\mathcal{D}(u, v) \mid (u, v) \in T\}$. Across the 56 cities, \mathcal{D}_C exhibits a peaked dis-
140 tribution with a mean of 7.45 ± 0.73 (see Figure 1c). Tokyo ranks as the city with the highest value
141 ($\mathcal{D}_{\text{Tokyo}} = 8.697$), while Mumbai has the lowest ($\mathcal{D}_{\text{Mumbai}} = 5.328$). Between these extremes, cities
142 display varying levels of \mathcal{D}_C (see Supplementary Note 2). For example, Rio de Janeiro, Rome,
143 and Madrid exhibit low DiverCity (5.620, 6.434, and 7.097); London, Chicago, and Sao Paulo
144 exhibit high DiverCity values (8.191, 8.283, and 8.369). Gridded cities, comprising approximately
145 40% of the sample (see Table 1), have higher and less variable \mathcal{D}_C scores (7.68 ± 0.55) compared
146 to non-gridded cities (7.29 ± 0.79). This is because gridded cities have near-shortest routes with
147 more similar travel times than non-gridded counterparts (see Supplementary Note 3).

148 We find that \mathcal{D}_C is a proxy for traffic efficiency: cities with higher \mathcal{D}_C values exhibit more
 149 evenly distributed traffic across road segments. Indeed, \mathcal{D}_C is negatively correlated with mean
 150 edge load (Pearson's correlation $r = -0.644$, Spearman's correlation $\rho = -0.665$, see Figure 1d),
 151 which reflects the frequency with which a road segment is traversed by routes in the network (see
 152 Methods for details).

153 The spatial analysis of $\mathcal{D}(u, v)$ reveals that it is not equally distributed within a city: it is low
 154 in the city center, with an average value of 5 within the first kilometer (Figure 1e), and increases
 155 sharply with distance from the center, stabilizing at around 7.5 beyond 10 km. This pattern reflects
 156 a rapid expansion of routing options in the near periphery, followed by a plateau. This trend is well
 157 captured ($R^2 = 0.93$) by a bounded exponential function: $y = \alpha \cdot e^{-\beta x} + \gamma$, where the parameter
 158 values are $\alpha = -6.93$, $\beta = -0.95$, and $\gamma = 7.70$ (red dashed curve in Figure 1e). An intriguing
 159 outlier deviates from the overall trend: $\mathcal{D}_{Rome}(u, v)$ has a marked decline between 10 and 12 km
 160 from the city center (see Figure 1e), coinciding with the location of Rome's major ring road.

161 This extreme case motivated us to investigate whether reductions in $\mathcal{D}(u, v)$ generally oc-
 162 cur near major mobility attractors across the cities under scrutiny. Here, we define mobility at-
 163 tractors as high-capacity transport infrastructures designed to facilitate and accelerate large traffic
 164 volumes, including highways, ring roads, and major arterial roads (see Methods for more de-
 165 tails). Drivers predominantly prefer mobility attractors over secondary roads^{41,42}, making it cru-
 166 cial to understand their impact on route diversification. For each sampled node i , we measure
 167 its distance to the nearest mobility attractor and calculate its node-level DiverCity as $\mathcal{D}(i) =$
 168 $\frac{1}{2(|N|-1)} \sum_{j \in N} (\mathcal{D}(i, j) + \mathcal{D}(j, i))$, i.e., the average trip DiverCity between i and all other sam-
 169 pled nodes j at the same radial distance (N). Figure 2 visualizes the spatial distribution of $\mathcal{D}(i)$ for
 170 two contrasting cities, Rome and Tokyo. In Rome (Figure 2a), low $\mathcal{D}_{Rome}(i)$ values (white and light
 171 blue areas) are strongly concentrated around Rome's ring road, which absorbs many routes and
 172 decreases route diversification within a 10–12 km radial band from the city center. In Tokyo (Fig-
 173 ure 2b), low $\mathcal{D}_{Tokyo}(i)$ values are scattered and typically associated with specific branches of major
 174 attractor roads rather than a single dominant feature. This distribution facilitates higher levels of

175 route diversification throughout the city.

176 To isolate the impact of mobility attractors on DiverCity, we analyze nodes located more
177 than 2 km from the city center. We exclude nodes within 2 km because $\mathcal{D}(i)$ is consistently low
178 in this range across all cities (as evident from Figure 1e), making it difficult to distinguish the
179 impact of mobility attractors from the inherent structural constraints of central areas. We find a
180 universal trend across all cities: on average, nodes with city-relative low $\mathcal{D}(i)$ – that is, in the lower
181 percentile ranges of their city’s $\mathcal{D}(i)$ distribution – consistently cluster nearby mobility attractors.
182 For instance, nodes in the bottom 10% of $\mathcal{D}(i)$ values are, on average, 1.33 km from the nearest
183 mobility attractor, significantly closer than the global average distance of 2 km and the 2.56 km
184 observed for nodes in the top 10% of $\mathcal{D}(i)$ values (Figure 2c). Mobility attractors funnel traffic
185 into a few paths, reducing potential route diversification for trips originating or ending nearby. This
186 effect weakens with distance, as sampled nodes farther from mobility attractors show progressively
187 higher $\mathcal{D}(i)$ values (see Figure 2c).

188 Our results also reveal that \mathcal{D}_C correlates with key road network features, including total road
189 length ($r = 0.561$, $\rho = 0.652$), the number of road intersections ($r = 0.431$, $\rho = 0.488$), and edge
190 circuitry, i.e., the extra distance relative to the straight line path ($r = -0.297$, $\rho = -0.415$). See
191 Supplementary Note 4 for a detailed analysis of \mathcal{D}_C ’s relationship with road network characteristics
192 and Table S1 for city-specific values. Notably, cities with higher \mathcal{D}_C have a higher density of
193 attractors and more evenly distributed attractors compared to cities with lower \mathcal{D}_C (see Figure
194 2d). We measure the density of attractors in a city as their total length per km^2 and their spatial
195 distribution using a dispersion index, H , computed as the average distance of a set of random
196 points to the nearest mobility attractor (see Methods for details). For instance, Tokyo, which has
197 the highest \mathcal{D}_C , features half the dispersion of attractors and double their density compared to
198 Mumbai, which ranks as the lowest in \mathcal{D}_C (Table 1). We present the DiverCity profiles and the
199 spatial distribution of $\mathcal{D}(i)$ for all the cities in Supplementary Note 6 (Figure S18-S73).

200 **Speed limits tuning on mobility attractors**

201 Mobility attractors are typically preferred by drivers because of their speed limits compared to
202 other roads⁴¹, absorbing a high volume of routes. This accelerates traffic flow but also limits
203 potential route diversification nearby. How can we curb the dominance of mobility attractors,
204 enhancing route diversification in their vicinity without compromising overall travel efficiency
205 across the city? We propose speed limit tuning as a strategic solution to address this challenge.

206 We simulate speed limit reductions ranging from 10% to 90% of original mobility attractors'
207 values. In the majority of cities under study, reducing speed limits lowers the dominance of attrac-
208 tors and increases \mathcal{D}_C . This relationship follows a bell-shaped trend, with the largest improvements
209 occurring at a 50% speed reduction (Figure 3a). Beyond this threshold, there is no advantage in
210 choosing the mobility attractors (too slow), yielding diminishing returns (\mathcal{D}_C improvement de-
211 creases). London exemplifies the typical DiverCity response to speed limit reductions: a 40%
212 reduction effectively eliminates the suppressive effects of mobility attractors, particularly those
213 located around 13 km and 30 km from the city center (see Figure 3d and Figure S45 for a detailed
214 visualization of attractors in London). Certain cities exhibit distinct DiverCity responses to speed
215 reductions (Figure 3a). For example, in Mumbai, speed reductions provide no benefits, while in
216 Lagos, a 20% speed reduction offers only a slight alleviation of the localized suppressive effects
217 of mobility attractors, while further reductions lead to a consistent decrease in DiverCity improve-
218 ments (Figure 3c). Rome and Brussels show instead the most significant improvements, with $\mathcal{D}_{\text{Rome}}$
219 peaking at a 70% speed reduction (+1.75) and $\mathcal{D}_{\text{Brussels}}$ reaching its highest increase at 80% speed
220 reduction (+1.4). Rome presents a particularly compelling case: the strong local impact of its ring
221 road, located approximately 11 km from the city center, gradually weakens as speed limits are
222 reduced (Figure 3e). As illustrated in Figure 4, under original speed limits, routes are heavily con-
223 centrated along the ring road, significantly suppressing route diversification (Figure 4a). However,
224 implementing a 40% speed reduction mitigates this effect, allowing alternative routes to emerge
225 and thereby increasing $\mathcal{D}_{\text{Rome}}$ (Figure 4b).

226 While speed reductions enhance potential route diversification, they also cause a moderate
227 increase in travel times. For instance, a 50% speed reduction results in trips that are five minutes
228 longer on average (Figure 3b). A 30% reduction yields notable benefits with minimal trade-offs: on
229 average, \mathcal{D}_C improves by 0.483 while travel times increase by two minutes only. Bridge-dominated
230 cities, such as San Francisco, New York City, and Rio de Janeiro, also present a distinctive pattern.
231 At speed reductions of up to 60%, these cities follow the global trend of moderate travel time
232 increases, but beyond this threshold, speed reductions lead to disproportionately large increases in
233 travel times. As shown in Figure 3b, at 80% reductions, travel time increases by 10 min in San
234 Francisco, 17 min in New York City, and 25 min in Rio de Janeiro, compared to a global average
235 of about 7 min. At 90% reductions, these values escalate further compared to the global average
236 of around 9 min: 18 min in San Francisco, 27 min in New York City, and an extreme increase of
237 48 min in Rio de Janeiro. Since bridges channel most routes between the two sides of these cities,
238 reducing their speed limits impacts travel times for all traversing routes. Moderate reductions
239 (< 60–70%) enhance \mathcal{D}_C with minimal travel time increases, but beyond this threshold, benefits
240 fade as travel times rise disproportionately.

241 **Simulations in a controlled setting**

242 To isolate the causal effects of the placement and speed limits of mobility attractors on DiverCity
243 in a controlled environment, we model a city as a uniform lattice L of intersections (nodes) and
244 road segments (edges), see Figure 5a. L spans an area of 60×60 km, matching the scale used for
245 real cities (a 30 km radius). Each road segment in L has a length of 500 meters and a default speed
246 limit of 50 km/h. We introduce mobility attractors in L as a “square” centered at L ’s midpoint,
247 with a side length of $2d$ and a speed limit of 100 km/h. We generate a set of trips using the radial
248 sampling method, following the same procedure applied to real cities. We then perform simulations
249 by varying the position and reducing the speed limits of mobility attractors while keeping the set
250 of trips fixed.

251 The simulation results confirm the findings observed for real cities. First, when L has no

mobility attractors, $\mathcal{D}_L(u, v)$ increases rapidly with distance from the city center before plateauing (see Figure 5b). Second, introducing a mobility attractor A_d at a distance d from the center of the lattice reduces $\mathcal{D}_L(u, v)$ in its vicinity, the extent of this reduction being independent of d and increasing with the speed limit A_d (see Supplementary Notes 5a and 5b). Sampled nodes in the lower percentile ranges of $\mathcal{D}_L(i)$ consistently cluster near attractors, as observed in real cities. For instance, for $d = 10$ km, low- $\mathcal{D}_L(i)$ nodes are, on average, just 0.85 km from the nearest attractor (Figure 5c). Third, the presence of multiple attractors stabilizes $\mathcal{D}_L(u, v)$ globally. Specifically, introducing a second attractor $B_{d+\delta}$ in an offset δ from A_d provides limited benefits near the center but becomes more effective farther from it (see Supplementary Note 5c). The benefit decreases linearly as δ increases, and this effect generalizes to larger configurations: attractors clustered farther from the grid center stabilize $\mathcal{D}_L(u, v)$ more effectively, with the benefit decreasing linearly as the offset increases (see Supplementary Note 5d). This behaviour is exemplified in Figure 5d, showing $\mathcal{D}_L(u, v)$ under three configurations. A single attractor at 10 km from the center sharply reduces $\mathcal{D}_L(u, v)$ nearby. Adding a second attractor at 11 km from the center improves DiverCity locally, while three clustered attractors (at 10, 11, and 12 km) stabilize and enhance $\mathcal{D}_L(u, v)$ globally.

Finally, as observed in real cities, reducing attractors' speed limits in L improves \mathcal{D}_L linearly until the attractor speed aligns with other roads, after which improvements plateau (Figure 5e). However, we identify a key discrepancy: in L , travel times increase linearly up to this equilibrium point (50%) and then stabilize, whereas in real cities, travel times continue to rise beyond equilibrium. This difference arises from the presence of bottlenecks in real cities, such as bridges, which remain critical even at reduced speed limits. To incorporate bottlenecks into L , we divide it into two unconnected regions connected by an attractor acting as a bridge (see Figure S17). In this modified setup, travel times continue to rise beyond equilibrium, closely mirroring the behavior of real cities (Figure 5f).

277 **Discussion**

278 Since mobility attractors draw traffic towards themselves, their spatial distribution affects potential
279 route diversification in their vicinity. Rome and Tokyo represent two contrasting examples of this
280 phenomenon: Rome, with its single dominant ring road, exhibits low DiverCity; Tokyo, with its
281 dense and widespread network of attractors, shows high DiverCity.

282 Our findings raise a critical question: Is high DiverCity always desirable for a city? Urban
283 planners typically design mobility attractors as primary traffic arteries, intentionally limiting route
284 diversity to minimize spillover onto local streets. DiverCity provides a quantitative measure to
285 evaluate how effectively road infrastructure attracts traffic to its surroundings and globally, en-
286 abling planners to distinguish between planned outcomes and unintended inefficiencies. While
287 mobility attractors are essential for ensuring fluidity of traffic within a city, their impact on route
288 diversification depends on how they are integrated into the road network. The distance of mobility
289 attractors from the city center, their spacing relative to one another, their distribution across the
290 road network, and their speed limits are all critical design factors that determine whether route di-
291 versification is enhanced or suppressed. Effective urban planning is not merely about constructing
292 high-speed roads but integrating them properly into the road network to trade off traffic fluidity
293 and potential route diversification. DiverCity supports simulations and scenario analyses, helping
294 identify optimal speed limit adjustments on attractors to maximize potential route diversification.
295 Supplementing this analysis with empirical data – such as vehicular GPS traces – could shed light
296 on the gap between a city’s potential route diversification and the actual routes drivers take on the
297 road network. This would help quantify both the potential influence of attractors and how drivers
298 capitalize on these opportunities in their everyday travel.

299 An intriguing direction emerging from our study is investigating the relationship between
300 route diversification and urban policies such as the 30 km/h City and the 15-minute City. The 30
301 km/h City concept promotes road safety by lowering speed limits to 30 km/h on all urban streets
302 except major roadways (i.e., mobility attractors). In cities where this policy has been implemented,

303 it led to a reduction of accidents and traffic while encouraging greater use of bicycles and public
304 transportation, with only a minor impact on travel times^{32,33}. However, the impact of the 30 km/h
305 policy on potential route diversification remains uncharted territory. Tools like those introduced in
306 this study could help simulate how drivers adjust their routes in response to the policy and identify
307 which roads would be affected by their alternative routes. Additionally, examining the interplay
308 between speed limit adjustments on mobility attractors and roads affected by the 30 km/h policy
309 could help identify optimal speed limit combinations that balance policy objectives, traffic flow,
310 and route diversification.

311 The 15-minute city model suggests that ensuring essential services and amenities are acces-
312 sible within a 15-minute walk or bike ride can improve efficiency, equity, and sustainability^{43,44}.
313 Recent research indicates that only a small fraction of cities worldwide meet these criteria^{12,45,46}.
314 Promoting route diversification – through strategies like speed limit adjustments, as proposed in
315 our work – can enhance connectivity between neighborhoods, improve access to essential services
316 and amenities, and serve as a practical step toward achieving the vision of a 15-minute city.

317 In conclusion, our study advances the understanding of vehicular routing in urban environ-
318 ments while illuminating its intricate ties to road network structure. Building on these insights, we
319 introduce practical, actionable tools to adapt and design road networks fostering diverse routes. At
320 the same time, our findings highlight the dual role of mobility attractors, offering rapid connec-
321 tions between city areas yet potentially suppressing alternative routes. By providing both a deeper
322 understanding and tangible methodologies for intervention, our research sparks further exploration
323 and equips urban planners to shape more equitable, resilient cities.

324 **Methods**

325 **Road Network Representation.** To analyze route diversification in urban road networks, we
326 used detailed representations of the road infrastructures in 56 global cities. Each city's road net-
327 work is modeled as a directed weighted multigraph $G = (V, E)$, where V denotes the set of nodes

328 v_i representing intersections, and E is a multiset of edges representing the road segments connect-
329 ing the vertices. Each edge $e_{i,j} \in E$ is associated with its minimum expected travel time, length,
330 capacity, and speed limit. To ensure consistency in our analysis, we defined the city center for
331 each urban area using geographic coordinates referenced from [latlong.net](#). We extracted the road
332 network of each city from OpenStreetMap⁴⁰ using OSMnx⁴⁷, centering it on the city's center and
333 extending approximately 30 km in radius. This distance encompasses a substantial portion of the
334 urban and peri-urban road network, allowing for a comprehensive evaluation of route diversifica-
335 tion within a broad geographic scope.

336 **Radial Sampling.** To systematically assess potential route diversification, we employed a radial
337 sampling approach to generate origin-destination (OD) pairs by scanning the network radially from
338 the city center. This method, widely used to analyze spatial metrics and urban patterns within cities
339^{29,31}, ensures a uniform distribution of OD pairs across varying distances from the city center,
340 facilitating a comprehensive evaluation of potential route diversification while avoiding sample
341 bias. We identified each city's center based on geographic coordinates sourced from [latlong.net](#).
342 From this center, we defined concentric circles with radii ranging from 1 km to 30 km at intervals
343 of 1 km, representing increasing distances from the urban core to the periphery. The maximum
344 radius of 30 km was chosen to sufficiently cover the urbanized areas of our sample cities^{29,31}.
345 Along each circle, we selected points at 10° intervals, yielding 36 equally spaced points along the
346 circumference. Each point was then matched to the nearest road network node within a distance
347 threshold of 500 m. Points that could not be matched –for example, those in inaccessible areas
348 such as water bodies, forests, or unconnected terrain– were excluded from the sample. In an ideal
349 scenario, where all points are successfully matched, this process generates up to 1,260 OD pairs
350 per radius, yielding a maximum of 37,800 OD pairs per city. However, the actual number of pairs
351 varies based on the city's topology and the accessibility of its road network.

352 **Near Shortest Routes (NSR).** To compute the near-shortest routes (NSR) between an origin-
353 destination (OD) pair, we perform two key steps:

354 **1. Generating Alternative Routes:** First, we generate k alternative routes using the Path Pe-
355 nalization (PP)^{48,49} algorithm, a widely used and robust alternative routing method that
356 forms the foundation for several advanced algorithms^{34–38}. This algorithm generates k alter-
357 native routes by iteratively penalizing the weights of edges contributing to the current fastest
358 path^{34,35,50,51}. Specifically, in each iteration, PP computes the fastest path and increases the
359 weights of its constituent edges by a factor p , such that $w(e) = w(e) \cdot (1 + p)$ ³⁴, where
360 $w(e)$ is the expected travel time of edge e . This penalization ensures that previously selected
361 edges become less likely to be chosen in subsequent iterations, prompting the exploration of
362 alternative routes. The penalization is cumulative, meaning that edges used in earlier iter-
363 ations are further penalized in subsequent iterations³⁴. The higher the penalty factor p , the
364 greater the deviation from the original fastest path⁵². In our experiments, we set $p = 0.1$,
365 and supplementary analyses show that results are consistent across a range of p values.

366 **2. Filtering Near Shortest Routes:** From the set of k generated routes, we identify the NSR
367 as the routes whose costs do not exceed the cost of the fastest route by more than $\epsilon\%$ ³⁶. This
368 ensures that the resulting routes are practical alternatives that are close in cost to the optimal
369 route. In our experiments, we set $\epsilon = 30\%$, allowing the NSRs to have costs up to 30%
370 higher than the fastest path. Supplementary analyses confirm that results remain consistent
371 for different values of ϵ .

372 We compute the spatial spread S of the NSR between an origin-destination pair (u, v) as
373 $\mathcal{S}(\text{NSR}(u, v)) = 1 - J(\text{NSR}(u, v))$, where J is the average weighted Jaccard similarity among all
374 pairs of routes in $\text{NSR}(u, v)$. The weighted Jaccard similarity⁵³ accounts for the length of each
375 road segment and is defined as: $J(A, B) = \frac{\sum_{e \in A \cap B} w_e}{\sum_{e \in A \cup B} w_e}$ where A and B are the routes represented as
376 sets of road segments, and w_e is the length of road segment e . A high $\mathcal{S}(\text{NSR}(u, v))$ value indicates
377 greater spatial spread, reflecting more diverse routing options. Conversely, a low value suggests

378 that the routes are geographically similar and significantly overlap.

379 **Mobility Attractors.** In our study, we define mobility attractors as high-capacity transport in-
380 frastructures designed to facilitate and accelerate large traffic volumes, including highways, ring
381 roads, and major arterial roads. To identify mobility attractors in each city, we employ a system-
382 atic approach using OpenStreetMap road network data. Our classification of mobility attractors
383 focused on two primary road types commonly designed to handle significant traffic volumes:

- **Motorways** (tag OSM: `motorway`): High-capacity, high-speed routes designed for fast, long-distance travel with limited access points.
- **Trunks** (tag OSM: `trunk`): Major roads connecting important regions, supporting significant traffic flow just below motorway levels.

388 The identification process allows us to capture the physical characteristics of these roads and their
389 intended role in traffic planning.

390 **Spatial Dispersion of Mobility Attractors.** To quantify the spatial dispersion of mobility at-
391 tractors across the geographical area of interest, we employ a sampling-based methodology. We
392 generate $N=20,000$ random points distributed uniformly within the area of interest while systemat-
393 ically excluding inaccessible regions such as water bodies, forests, and other non-urbanized zones.
394 For each randomly generated point, we compute the distance H to the nearest mobility attractor.
395 The distance metric for each city is then defined as the average of these distances. Lower values
396 indicate a more uniform and dense distribution of attractors, implying high coverage and accessi-
397 bility. Conversely, higher values suggest a sparse and uneven distribution of attractors, pointing to
398 limited coverage and diminished accessibility in specific areas.

399 **Edge Load.** The edge load serves as a proxy for the number of routes likely to traverse individual
400 road segments. For each trip in T , we distribute one traffic unit evenly across its near-shortest
401 routes (NSRs). If a trip has n NSRs, each route receives a traffic load of $\frac{1}{n}$, which is then added to
402 every edge it traverses. This process is repeated for all trips, accumulating traffic loads across the
403 network.

404 To assess city-wide traffic distribution, we compute the mean edge load by averaging the
405 edge loads of all road segments traversed by at least one route. A low mean edge load indicates
406 that routes are distributed more evenly across the network. Conversely, a high mean edge load
407 suggests that routes are concentrated on a smaller subset of road segments.

408 For cross-city comparisons, we normalize edge loads by dividing them by the total number
409 of trips ($|T|$) before averaging, ensuring comparability across cities with different numbers of trips.

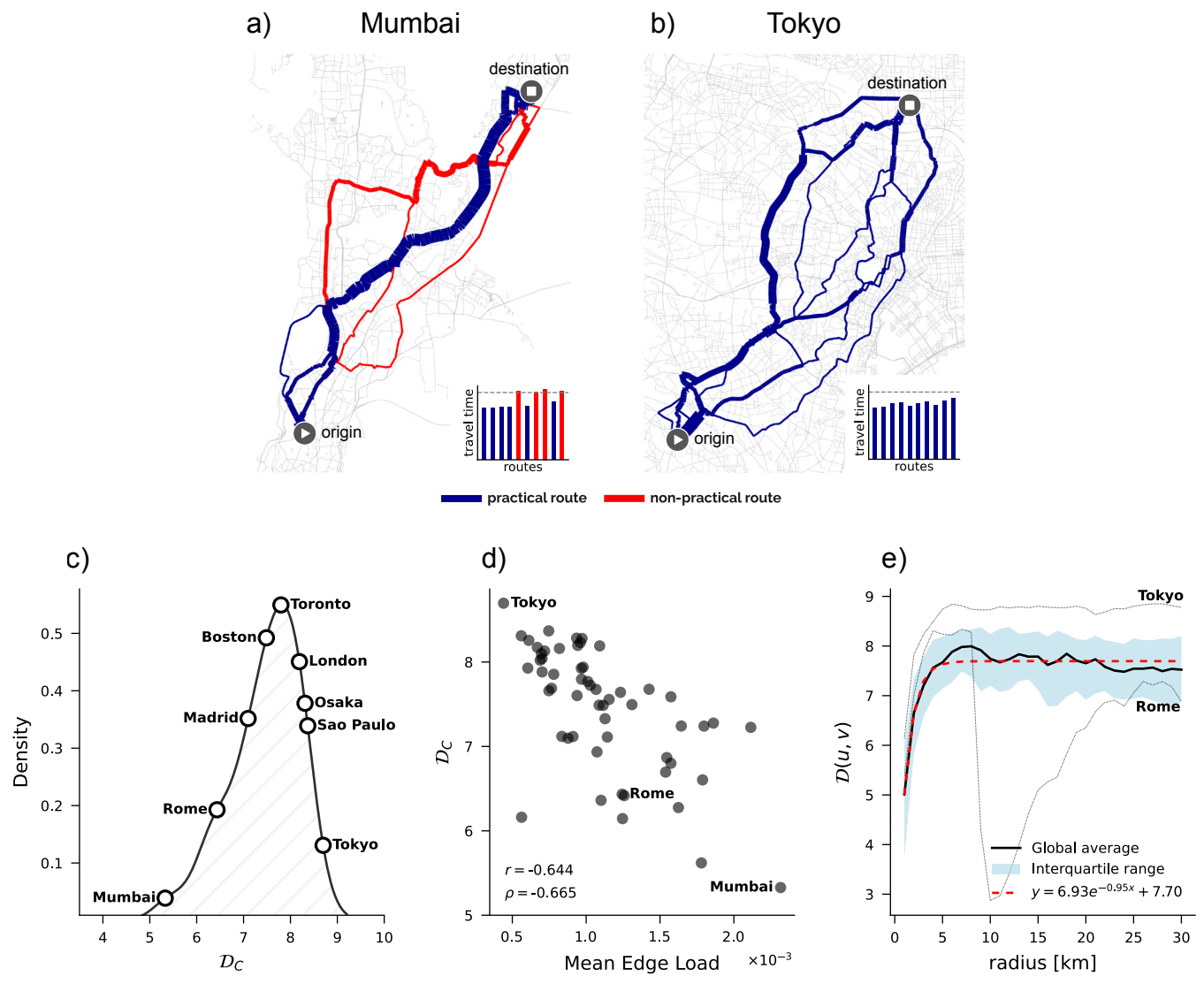


Figure 1

410 **Figure 1. Overview of DiverCity and global patterns in urban road networks.** **(a)** Example
411 of a trip with low DiverCity (2.18) in Mumbai. Near-shortest routes significantly overlap, leading
412 to a low route diversity. **(b)** Example of a trip with high DiverCity (9) in Tokyo, characterized
413 by multiple spatially diverse near-shortest routes. For panels (a) and (b), inset bar plots show the
414 travel time of each alternative route, with NSRs in blue and non-feasible routes (exceeding the near-
415 shortest threshold, shown as a dashed line) in red. **(c)** Distribution of median DiverCity across 56
416 cities, highlighting substantial variability. **(d)** Median DiverCity versus average normalized edge
417 load, showing how greater route diversity correlates with more efficient traffic distribution. **(e)**
418 DiverCity for trips at varying radial distances from the city center. The black line shows the global
419 average, the light blue area represents the interquartile range, and the red line is an exponential fit
420 ($R^2 = 0.93$). Deviations include Tokyo's high values and Rome's localized drop near its ring road.

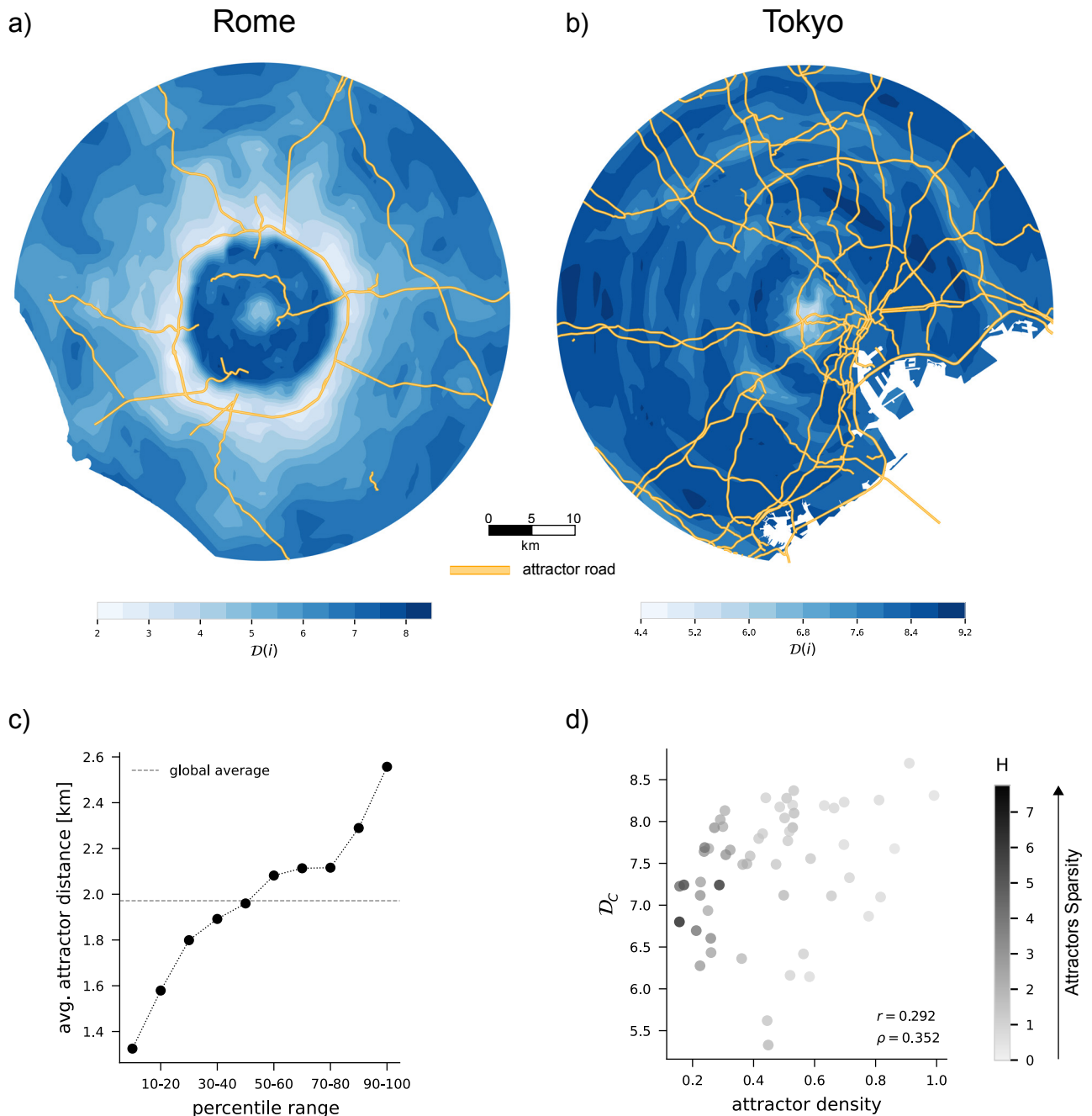


Figure 2

421 **Figure 2. DiverCity and mobility attractors.** (a, b) Spatial distribution of node-level DiverCity,
422 $\mathcal{D}(i)$, in Rome (a) and Tokyo (b). Values are interpolated between nodes, with mobility attractors
423 highlighted in orange. Low- $\mathcal{D}(i)$ areas are represented in light blue, while high- $\mathcal{D}(i)$ areas are
424 shown in dark blue, following the color gradient in the scale. Rome exhibits generally lower $\mathcal{D}(i)$
425 values and sparser attractors compared to Tokyo. In both cities, areas with low $\mathcal{D}(i)$ (relative to the
426 city's distribution) tend to cluster around mobility attractors. In Rome, low $\mathcal{D}(i)$ areas are strongly
427 concentrated near the city's major ring road, while in Tokyo, they are distributed around branches
428 of nearby mobility attractors, though less prominently than in Rome. (c) The average distance to
429 the nearest attractor for nodes in different percentile ranges of $\mathcal{D}(i)$ within their respective cities.
430 Nodes with lower $\mathcal{D}(i)$ are consistently closer to attractors. The dashed line represents the global
431 average distance across all cities. (d) The relationship between city-level DiverCity (\mathcal{D}_C) and
432 attractor density. Each point corresponds to a city, with color intensity indicating attractor spatial
433 dispersion (H). Cities with denser and more evenly distributed attractors tend to have higher \mathcal{D}_C .

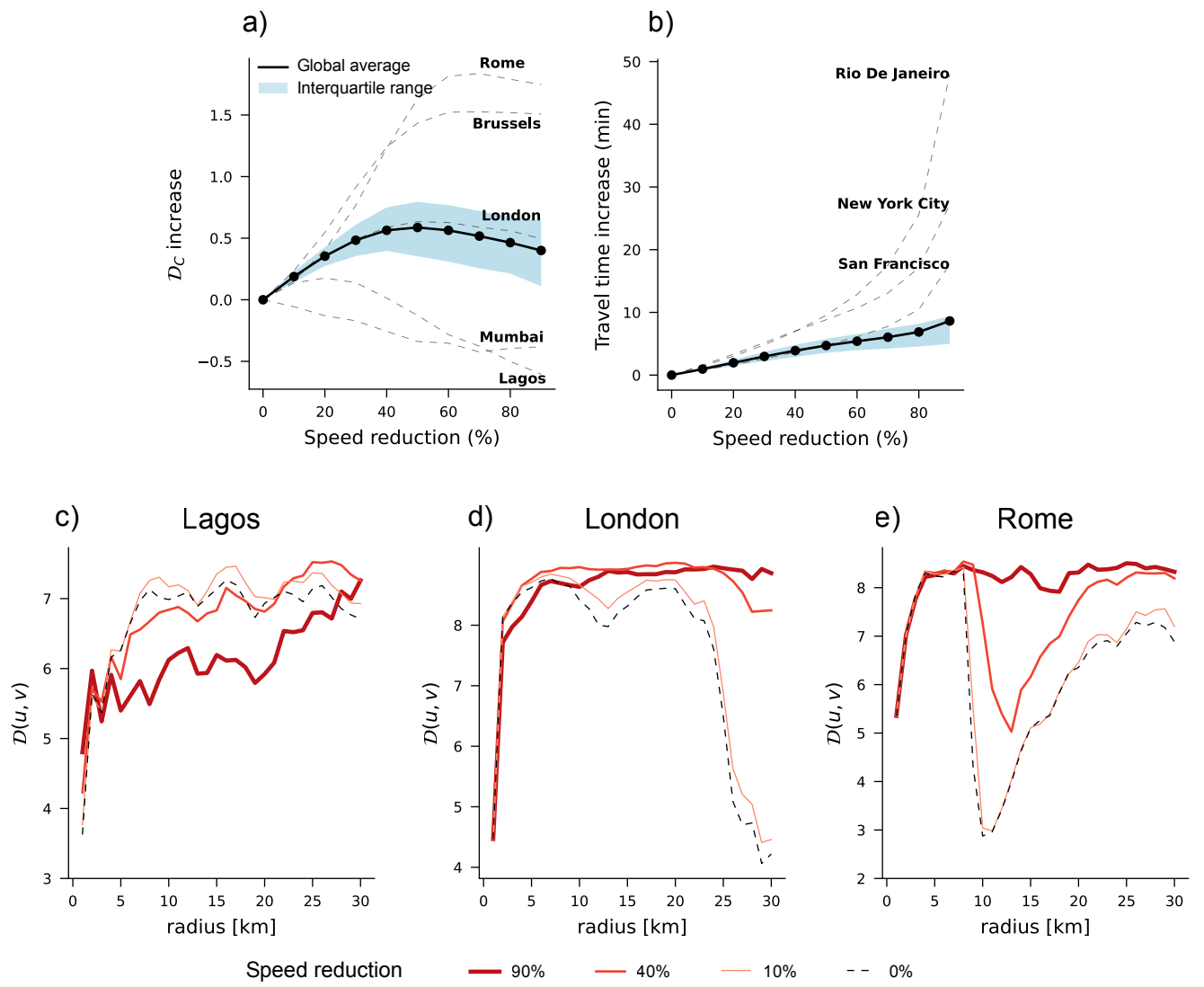


Figure 3

434 **Figure 3. Impact of speed limit tuning.** **(a)** Effect of speed reductions on DiverCity. Cities
435 such as Rome and Brussels show strong \mathcal{D}_C improvements, while London follows the global trend
436 with a peak at around 50% speed reduction before stabilizing. In contrast, Mumbai and Lagos
437 exhibit limited or negative effects. **(b)** Effect of speed reductions on travel time. Cities with critical
438 mobility bottlenecks (e.g., bridges in Rio de Janeiro, New York City, and San Francisco) experience
439 disproportionately large increases in travel times beyond a 50% speed reduction. In panels (a) and
440 (b), black lines represent the global average across all cities, while the blue shaded areas denote
441 the interquartile range. **(c-e)** DiverCity for trips at varying radial distances for: **(c)** Lagos, where
442 speed reductions negatively impact route diversification, **(d)** London, where DiverCity increases
443 with speed reductions before stabilizing at 50% as the localized effect of attractors decreases, and
444 **(e)** Rome, where reductions mitigate the localized dominance of mobility attractors such as the
445 ring road. Speed reduction scenarios (in shades of red) are compared to the baseline case (black
446 dotted line).

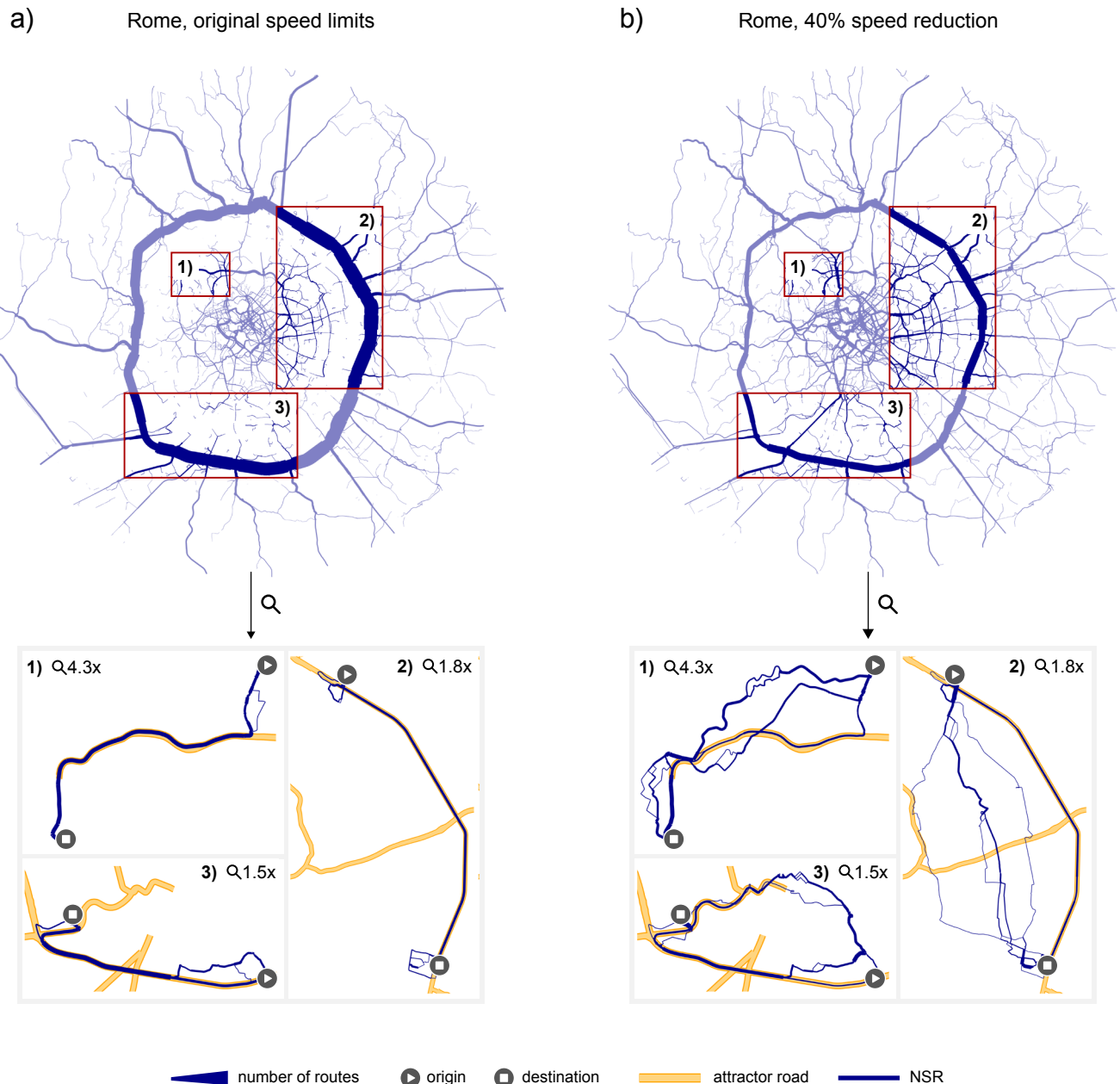


Figure 4

447 **Figure 4. Speed limit tuning in Rome.** Traffic distribution in Rome under original speed limits
448 **(a)** and after a 40% speed reduction **(b)**. The width of each road segment is proportional to the
449 number of near-shortest routes traversing it, based on the set of sampled trips T . Under original
450 speed limits, routes are highly concentrated on the ring road, suppressing potential route diversity.
451 After a 40% speed reduction, routes are more evenly distributed, reducing reliance on the ring road
452 and enabling alternative routes to emerge. For each scenario, inset plots (1–3) focus on specific
453 regions (highlighted in red on the map), providing magnified views of selected origin-destination
454 pairs near and inside mobility attractor roads (shown in orange). The magnification factors are
455 indicated in each inset. Under original speed limits (a), all alternative routes are funneled into the
456 ring road, limiting route diversification. With speed reductions (b), fewer routes rely on the ring
457 road, enabling alternative routes to emerge, increasing spatial diversity, and revealing previously
458 “hidden” routes.

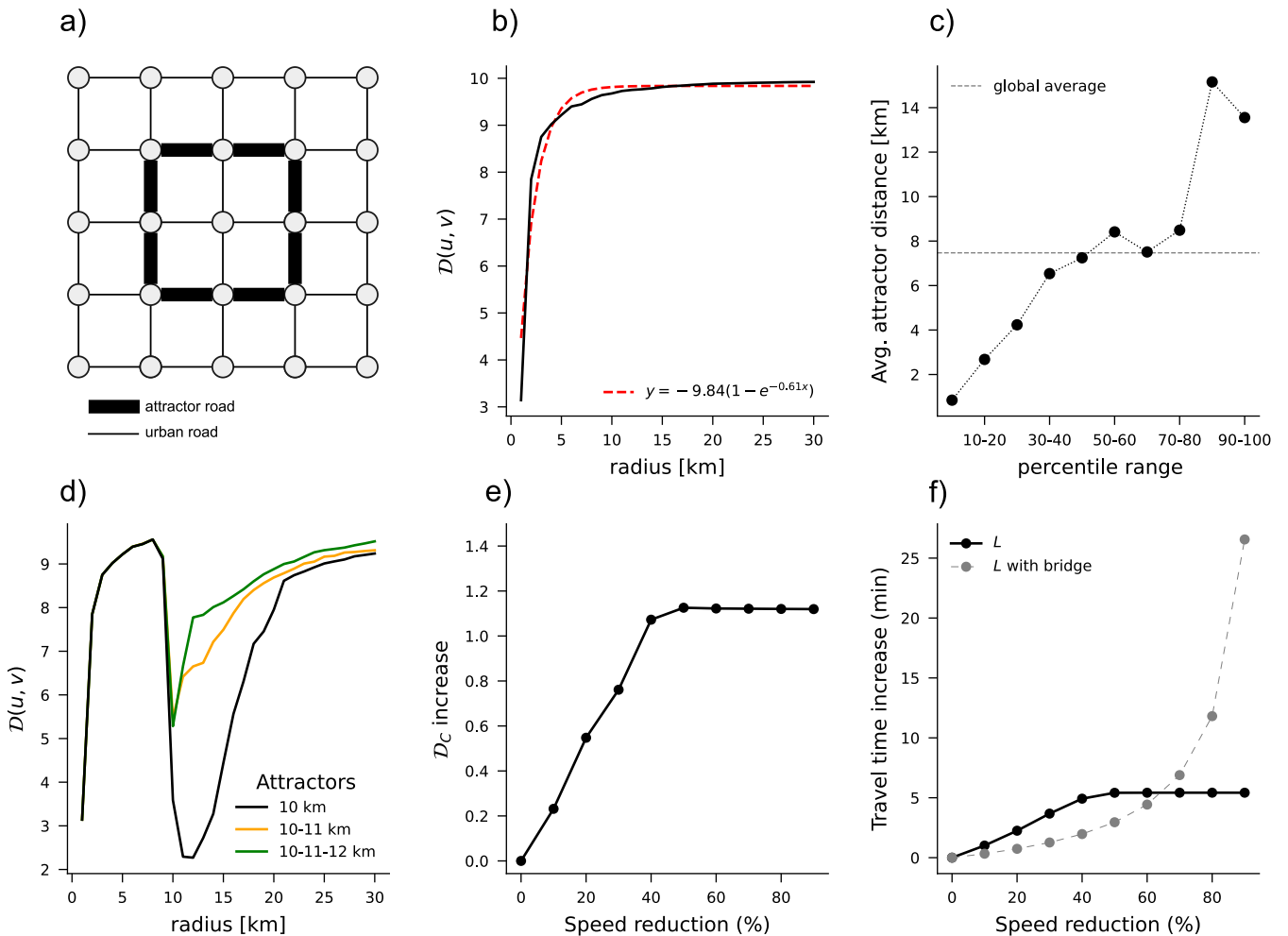


Figure 5

459 **Figure 5. Simulations in a controlled setting.** (a) Illustration of the lattice grid model L , where
460 intersections are represented as nodes and roads as edges. Thicker edges indicate mobility at-
461 tractors with higher speed limits, while the remaining edges represent standard urban roads. (b)
462 DiverCity, $\mathcal{D}(u, v)$, as a function of radial distance from the center of the lattice. Without mobility
463 attractors, $\mathcal{D}(u, v)$ increases rapidly near the center and plateaus farther out, following a bounded
464 exponential trend (red dashed line, $R^2 = 0.93$). (c) The average distance to the nearest attractor for
465 nodes grouped by percentile ranges of $\mathcal{D}(i)$ in the lattice model. Nodes with lower $\mathcal{D}(i)$ are con-
466 sistently closer to attractors, mirroring the trends observed in real-world road networks. (d) The
467 effect of introducing attractors at varying distances from the center on $\mathcal{D}(u, v)$. A single attractor at
468 10 km sharply reduces $\mathcal{D}(u, v)$ near its location. Adding more attractors at greater distances (e.g.,
469 10–12 km) helps stabilize and increase $\mathcal{D}(u, v)$ globally. (e) The effect of speed limit reductions on
470 city-level DiverCity (\mathcal{D}_C) in the lattice. Reducing attractor speeds increases \mathcal{D}_C , with the largest
471 improvements at around 50% speed reduction. Further reductions yield diminishing returns as at-
472 tractors lose their dominance. (f) The impact of speed limit reductions on average travel time. For
473 a simple lattice (L), travel time rises modestly with reductions. However, introducing a bridge-like
474 bottleneck significantly amplifies travel time increases at higher speed reductions, reflecting the
475 trend observed for real-world road networks.

rank	City	\mathcal{D}_C	attractors length	attractors density	H [km]	Pop. Density	rank	City	\mathcal{D}_C	attractors length	attractors density	H [km]	Pop. Density
1	Tokyo	8.697	2,534	0.910	1,339	6,169	29	Detroit	7.603	844	0.309	3,761	1,750
2	Sao Paulo	8.369	1,652	0.532	2,215	8,055	30	Vancouver	7.588	481	0.389	2,383	5,493
3	Osaka	8.311	2,808	0.992	1,064	12,111	31	Sydney	7.557	1,042	0.587	2,097	400
4	Chicago	8.283	799	0.440	1,769	4,663	32	Bangkok	7.495	1,155	0.378	2,642	5,293
5	Melbourne	8.279	1,282	0.508	2,249	500	33	San Francisco	7.489	753	0.474	2,154	7,171
6	New York City	8.257	2,128	0.811	1,381	11,316	34	Boston	7.487	950	0.364	2,784	5,200
7	Shanghai	8.231	2,012	0.697	1,422	3,922	35	Tehran	7.328	1,578	0.714	1,617	12,028
8	Philadelphia	8.197	1,680	0.528	1,602	4,129	36	Hamburg	7.277	683	0.226	3,380	2,366
9	London	8.191	2,012	0.632	1,363	5,614	37	Bogota	7.242	441	0.172	6,510	5,018
10	Los Angeles	8.174	1,278	0.486	1,762	3,287	38	Manila	7.241	553	0.288	7,162	41,515
11	Seoul	8.161	2,068	0.664	1,563	16,552	39	Ottawa	7.226	428	0.158	5,414	334
12	New Delhi	8.130	960	0.306	2,836	11,289	40	Jakarta	7.119	1,225	0.499	2,634	15,292
13	Mexico City	8.099	1,580	0.533	2,520	6,202	41	Athens	7.117	425	0.225	3,854	17,040
14	Houston	8.042	1,574	0.502	2,110	1,497	42	Kuala Lumpur	7.111	1,620	0.655	2,100	7,276
15	Buenos Aires	8.022	510	0.291	3,044	15,046	43	Madrid	7.097	1,833	0.816	1,359	5,390
16	Milan	7.939	932	0.299	2,941	7,700	44	Brussels	6.935	800	0.250	3,016	7,489
17	Cairo	7.928	1,499	0.528	2,636	3,256	45	Shenzhen	6.868	1,798	0.777	1,244	8,534
18	Lima	7.926	432	0.272	3,756	3,329	46	Kinshasa	6.801	209	0.157	7,749	1,713
19	Dallas	7.883	1,622	0.518	1,832	1,525	47	Lagos	6.696	439	0.212	5,108	6,871
20	Paris	7.854	1,341	0.430	1,906	20,460	48	Dhaka	6.604	780	0.260	4,226	30,460
21	Toronto	7.796	740	0.417	2,009	4,336	49	Rome	6.434	741	0.261	3,309	2,232
22	Washington D.C.	7.769	1,620	0.512	1,976	3,969	50	Barcelona	6.417	870	0.564	1,812	15,980
23	Beijing	7.724	2,218	0.696	1,273	1,334	51	Amsterdam	6.362	898	0.361	2,642	5,265
24	Karachi	7.689	416	0.240	4,733	26,629	52	Moscow	6.276	688	0.224	3,654	5,257
25	Berlin	7.677	722	0.253	3,063	4,227	53	Istanbul	6.161	996	0.520	1,649	2,987
26	Guangzhou	7.676	2,749	0.862	1,035	2,512	54	Dubai	6.145	939	0.583	1,294	860
27	Santiago	7.660	679	0.323	3,271	10,748	55	Rio De Janeiro	5.620	796	0.445	2,314	5,340
28	Cape Town	7.641	322	0.238	3,842	1,530	56	Mumbai	5.328	739	0.448	2,652	20,694

Table 1: City-level DiverCity ranking. The table presents a comparative analysis of 56 cities, ranked by their city-level DiverCity (\mathcal{D}_C). For each city, we include the total length of mobility attractors (e.g., highways, major roads), their density (defined as attractor length per km²), the spatial dispersion of attractors (H), and the city’s population density. A \blacksquare symbol next to the city name indicates that the city exhibits a gridded road network structure.

Acknowledgements We thank Daniele Fadda for his precious support with data visualization and Giovanni Mauro, Minho Kim, Margherita Lalli, Antonio Desiderio, Daniele Gambetta, Gabriele Barlacchi, and Charlotte Brumont for their useful suggestions. LP and GC have been partially supported by: PNRR (Piano Nazionale di Ripresa e Resilienza) in the context of the research program 20224CZ5X4 PE6 PRIN 2022 “URBAI – Urban Artificial Intelligence” (CUP B53D23012770006), funded by the European Commission under the Next Generation EU programme. DP has been partially supported by PNRR - M4C2 - Investimento 1.3, Partenariato Esteso PE00000013 - ”FAIR – Future Artificial Intelligence Research” – Spoke 1 “Human-centered AI”, funded by the European Commission under the NextGeneration EU programme. MN has been partially supported by Project “SoBigData.it - Strengthening the Italian RI for Social Mining and Big Data Analytics”, prot. IR0000013, avviso n. 3264 on 28/12/2021.

Data availability statement This study relies solely on road network data extracted from OpenStreetMap⁴⁰ using OSMnx⁴⁷. The Python code used to download the road networks for the cities analyzed in this work is publicly available at <https://github.com/GiulianoCornacchia/DiverCity>.

Code availability statement The Python code required to fully reproduce the analyses presented in this study is publicly available at <https://github.com/GiulianoCornacchia/DiverCity>.

Author contributions GC conceptualized the study, developed the code of measures and experiments, conducted all experiments, designed and created the figures, developed the online platform, and wrote the manuscript. LP conceptualized the study, designed the experiments, designed the figures, wrote the manuscript, and supervised the research. MN and DP conceptualized the study and critically revised the manuscript. MG conceptualized the study, designed the experiments, wrote the manuscript, and supervised the research. All authors reviewed and approved the final version of the manuscript.

Competing interests The authors declare no competing interests.

References

1. Saberi, M. *et al.* A simple contagion process describes spreading of traffic jams in urban networks. *Nature communications* **11**, 1616 (2020).
2. Çolak, S., Lima, A. & González, M. C. Understanding congested travel in urban areas. *Nat. Commun.* **7**, 1–8 (2016).
3. Zhang, L. *et al.* Scale-free resilience of real traffic jams. *Proceedings of the National Academy of Sciences* **116**, 8673–8678 (2019).
4. Xie, F. & Levinson, D. Measuring the structure of road networks. *Geographical Analysis* **39**, 336–356 (2007). URL <https://onlinelibrary.wiley.com/doi/abs/10.1111/j.1538-4632.2007.00707.x>. <https://onlinelibrary.wiley.com/doi/pdf/10.1111/j.1538-4632.2007.00707.x>.
5. Bohm, M., Nanni, M. & Pappalardo, L. Gross polluters and vehicle emissions reduction. *Nature Sustainability* **5**, 1–9 (2022).
6. Xu, X., Chen, A. & Yang, C. A review of sustainable network design for road networks. *KSCE Journal of Civil Engineering* **20**, 1084–1098 (2016). URL <https://www.sciencedirect.com/science/article/pii/S1226798824038741>.
7. Tenkanen, H., Pereira, R. H. M., Arcaute, E. & Gonzalez, M. C. Advances in geospatial approaches to transport networks and sustainable mobility. *Environment and Planning B: Urban Analytics and City Science* **50**, 2009–2016 (2023). URL <https://doi.org/10.1177/23998083231207768>.
8. Zeng, C., Zhao, Z., Wen, C., Yang, J. & Lv, T. Effect of complex road networks on intensive land use in china’s beijing-tianjin-hebei urban agglomeration. *Land* **9** (2020). URL <https://www.mdpi.com/2073-445X/9/12/532>.
9. Barthélemy, M. Spatial networks. *Physics Reports* **499**, 1–101 (2011). URL <https://www.sciencedirect.com/science/article/pii/S037015731000308X>.

10. Barthelemy, M. & Boeing, G. A Review of the Structure of Street Networks. *Findings* (2024).
11. Tsigdinos, S., Paraskevopoulos, Y., Tzouras, P., Bakogiannis, E. & Vlastos, T. Rethinking road network hierarchy towards new accessibility perspectives. *Transportation Research Procedia* **69**, 195–202 (2023). URL <https://www.sciencedirect.com/science/article/pii/S2352146523001722>. AIIT 3rd International Conference on Transport Infrastructure and Systems (TIS ROMA 2022), 15th-16th September 2022, Rome, Italy.
12. Bruno, M., Monteiro Melo, H. P., Campanelli, B. & Loreto, V. A universal framework for inclusive 15-minute cities. *Nature Cities* 1–9 (2024).
13. Wang, P., Hunter, T., Bayen, A. M., Schechtner, K. & González, M. C. Understanding road usage patterns in urban areas. *Scientific Reports* **2**, 1001 (2012).
14. Toole, J. L. *et al.* The path most traveled: Travel demand estimation using big data resources. *Transportation Research Part C: Emerging Technologies* **58**, 162–177 (2015). URL <https://www.sciencedirect.com/science/article/pii/S0968090X15001631>.
15. Wang, P., Liu, L., Li, X., Li, G. & González, M. C. Empirical study of long-range connections in a road network offers new ingredient for navigation optimization models. *New Journal of Physics* **16**, 13012 (2014). URL <https://dx.doi.org/10.1088/1367-2630/16/1/013012>.
16. Chen, R. *et al.* Scaling law of real traffic jams under varying travel demand. *EPJ Data Science* **13** (2024).
17. Zeng, W., Miwa, T. & Morikawa, T. Prediction of vehicle co2 emission and its application to eco-routing navigation. *Transportation Research Part C: Emerging Technologies* **68**, 194–214 (2016). URL <https://www.sciencedirect.com/science/article/pii/S0968090X16300110>.
18. Barth, M. & Boriboonsomsin, K. Real-world carbon dioxide impacts of traffic congestion. *Transportation research record* **2058**, 163–171 (2008).

19. Macfarlane, J. Your navigation app is making traffic unmanageable. *IEEE Spectrum* 22–27 (2019).
20. Siuhi, S. & Mwakalonge, J. Opportunities and challenges of smart mobile applications in transportation. *Journal of Traffic and Transportation Engineering* **3**, 582–592 (2016).
21. Schade, E., Savino, G.-L., Gunal, Y. & Schöning, J. Traffic jam by gps: A systematic analysis of the negative social externalities of large-scale navigation technologies. *PLoS one* **19**, e0308260 (2024).
22. Cornacchia, G., Nanni, M., Pedreschi, D. & Pappalardo, L. Navigation services amplify concentration of traffic and emissions in our cities. *arXiv preprint arXiv:2407.20004* (2024).
23. Cornacchia, G. *et al.* How routing strategies impact urban emissions. In *Proceedings of the 30th International Conference on Advances in Geographic Information Systems*, 1–4 (2022).
24. Pappalardo, L., Manley, E., Sekara, V. & Alessandretti, L. Future directions in human mobility science. *Nature Computational Science* (2023). URL <https://doi.org/10.1038/s43588-023-00469-4>.
25. Pedreschi, D. *et al.* Human-ai coevolution (2024). 2306.13723.
26. Pappalardo, L. *et al.* A survey on the impact of ai-based recommenders on human behaviours: methodologies, outcomes and future directions (2024). URL <https://arxiv.org/abs/2407.01630>. 2407.01630.
27. Freeman, L. C. A set of measures of centrality based on betweenness. *Sociometry* 35–41 (1977).
28. Levinson, D. & El-Geneidy, A. The minimum circuity frontier and the journey to work. *Regional Science and Urban Economics* **39**, 732–738 (2009). URL <https://www.sciencedirect.com/science/article/pii/S0166046209000660>.

29. Lee, M., Cheon, S., Son, S.-W., Lee, M. J. & Lee, S. Exploring the relationship between the spatial distribution of roads and universal pattern of travel-route efficiency in urban road networks. *Chaos, Solitons & Fractals* **174**, 113770 (2023). URL <https://www.sciencedirect.com/science/article/pii/S0960077923006719>.
30. Wang, S., Bette, H. M., Schreckenberg, M. & Guhr, T. How much longer do you have to drive than the crow has to fly? *npj Complexity* **1**, 1–9 (2024).
31. Lee, M., Barbosa, H., Youn, H., Holme, P. & Ghoshal, G. Morphology of travel routes and the organization of cities. *Nature communications* **8**, 2229 (2017).
32. Yannis, G. & Michelaraki, E. Review of city-wide 30 km/h speed limit benefits in europe. *Sustainability* **16**, 4382 (2024).
33. Tettamanti, T., Varga, B., Rottenstreich, O. & Emanuel, D. On the relationship of speed limit and Co2 emissions in urban traffic (2024).
34. Cheng, D., Gkountouna, O., Züfle, A., Pfoser, D. & Wenk, C. Shortest-path diversification through network penalization: A washington dc area case study. In *Proceedings of the 12th ACM SIGSPATIAL International Workshop on Computational Transportation Science*, 1–10 (2019).
35. Li, L., Cheema, M. A., Lu, H., Ali, M. E. & Toosi, A. N. Comparing alternative route planning techniques: A comparative user study on melbourne, dhaka and copenhagen road networks (extended abstract). In *2022 IEEE 38th International Conference on Data Engineering (ICDE)*, 1555–1556 (2022).
36. Häcker, C., Bouros, P., Chondrogiannis, T. & Althaus, E. Most diverse near-shortest paths. In *Proceedings of the 29th International Conference on Advances in Geographic Information Systems*, 229–239 (2021).
37. Cornacchia, G., Nanni, M. & Pappalardo, L. One-shot traffic assignment with forward-looking penalization. In *Proceedings of the 31st ACM International Conference on Advances in Geographic Information Systems*, 1–10 (2023).

38. Cornacchia, G., Lemma, L. & Pappalardo, L. Alternative routing based on road popularity. In *Proceedings of the 2nd ACM SIGSPATIAL Workshop on Sustainable Urban Mobility*, SUMob '24, 14–17 (Association for Computing Machinery, New York, NY, USA, 2024). URL <https://doi.org/10.1145/3681779.3696836>.
39. Lima, A., Stanojevic, R., Papagiannaki, D., Rodriguez, P. & Gonzalez, M. C. Understanding individual routing behaviour. *Journal of The Royal Society Interface* **13**, 20160021 (2016).
40. OpenStreetMap contributors. Planet dump retrieved from <https://planet.osm.org> . <https://www.openstreetmap.org> (2017).
41. Thomas, T. & Tutert, B. Route choice behavior in a radial structured urban network: Do people choose the orbital or the route through the city center? *Journal of transport geography* **48**, 85–95 (2015).
42. Ramming, M. S. Network knowledge and route choice. *Unpublished Ph. D. Thesis, Massachusetts Institute of Technology* **20** (2001).
43. Moreno, C., Allam, Z., Chabaud, D., Gall, C. & Pratlong, F. Introducing the “15-minute city”: Sustainability, resilience and place identity in future post-pandemic cities. *Smart cities* **4**, 93–111 (2021).
44. Lima, F. T. & Costa, F. The quest for proximity: A systematic review of computational approaches towards 15-minute cities. *Architecture* **3**, 393–409 (2023).
45. Yang, J. Visualizing and assessing the 15-minute city facility configuration of city region a study on the beijing-tianjin-hebei urban agglomeration. *Advances in Education, Humanities and Social Science Research* **4**, 63 (2023).
46. Vale, D. & Lopes, A. S. Accessibility inequality across europe: a comparison of 15-minute pedestrian accessibility in cities with 100,000 or more inhabitants. *npj Urban Sustain* **3** (2023).
47. Boeing, G. Osmnx: New methods for acquiring, constructing, analyzing, and visualizing complex street networks. *Computers, environment and urban systems* **65**, 126–139 (2017).

48. Johnson, P. E., Joy, D. S., Clarke, D. B. & Jacobi, J. M. Highway 3. 1: An enhanced highway routing model: Program description, methodology, and revised user's manual. Tech. Rep., Oak Ridge National Lab. (ORNL), Oak Ridge, TN (United States) (1993). URL <https://www.osti.gov/biblio/6549364>.
49. Ruphail, N., Ranjithan, S., ElDessouki, W., Smith, T. & Brill, E. A decision support system for dynamic pre-trip route planning. applications of advanced technologies. In *Transportation engineering: proceedings of the fourth international conference*, 325–329 (1995).
50. Akgün, V., Erkut, E. & Batta, R. On finding dissimilar paths. *European Journal of Operational Research* **121**, 232–246 (2000). URL <https://www.sciencedirect.com/science/article/pii/S0377221799002143>.
51. Bader, R., Dees, J., Geisberger, R. & Sanders, P. Alternative route graphs in road networks. In Marchetti-Spaccamela, A. & Segal, M. (eds.) *Theory and Practice of Algorithms in (Computer) Systems*, 21–32 (Springer Berlin Heidelberg, Berlin, Heidelberg, 2011).
52. Kobitzsch, M., Radermacher, M. & Schieferdecker, D. Evolution and Evaluation of the Penalty Method for Alternative Graphs. In Frigioni, D. & Stiller, S. (eds.) *13th Workshop on Algorithmic Approaches for Transportation Modelling, Optimization, and Systems*, vol. 33 of *Open Access Series in Informatics (OASIcs)*, 94–107 (Schloss Dagstuhl – Leibniz-Zentrum für Informatik, Dagstuhl, Germany, 2013). URL <https://drops-dev.dagstuhl.de/entities/document/10.4230/OASIcs.ATMOS.2013.94>.
53. da F. Costa, L. Further generalizations of the jaccard index. *CoRR* **abs/2110.09619** (2021). URL <https://arxiv.org/abs/2110.09619>.